NUMERICAL MODELING OF SUPERSONIC TWO-PHASE JET FLOWS WITH EXPLICIT SEPARATION OF SHOCK WAVES

É. I. Vitkin, L. T. Perel'man, and Yu. V. Khodyko

UDC 532.529

A two-phase supersonic jet issuing into a cotraveling flow is considered. The spatial distributions and temperature fields of the solid and liquid phases are investigated, taking account of the shock-wave structure of the underexpanded jet.

Formulation of the Problem

In a supersonic gas jet issuing from a Laval's nozzle, solid or liquid particles of size oscillating within the range from fractions of a micron to tens of microns may be present. The distribution of these particles in space and their characteristics depend strongly on the structure of the initial section of the jet; with increase in particle concentration, they themselves begin to influence the parameters of the gas close to the nozzle outlet and the geometry of the first "barrel."

The structure of two-phase flows in both nozzles and jets has been investigated, in particular, in [1-4], where the highly impressive methods of continuous calculation were used to calculate the flow parameters. The calculation scheme of the method of [5] is somewhat modified here in order to model the behavior of particles in the jet in a wide range of the parameters, explicitly separating the flow tubes in which no density discontinuities appear and those including the density discontinuities themselves.

The problem reduces to integration of the system of equations describing the motion and interaction of an ideal gas and a model "gas of particles"; the pressure in the latter is assumed to be zero. In particular, for an axisymmetric jet, the system of equations takes the form

$$\begin{gathered}
\frac{\partial}{\partial z}(\rho_i u_i)+\frac{\partial}{\partial r}(\rho_i v_i)+\frac{\rho_i v_i}{r}=0,\\
\frac{\partial}{\partial z}(\rho_i u_i^2+\delta_{1i}p)+\frac{\partial}{\partial r}(\rho_i u_i v_i)+\frac{\rho_i u_i v_i}{r}=f(u_j-u_i),\\
\frac{\partial}{\partial z}(\rho_i u_i v_i)+\frac{\partial}{\partial r}(\rho_i v_i^2+\delta_{1i}p)+\frac{\rho_i v_i^2}{r}=f(v_j-v_i),\\
\frac{\partial}{\partial z}(u_i e_i)+\frac{\partial}{\partial r}(v_i e_i)+\frac{v_i e_i}{r}=g(T_j^*-T_i^*)+\delta_{1i}f[(u_j-u_i)u_i+(v_j-v_i)v_i].
\end{gathered} \tag{1}$$

Here $i = 1, 2$ for the gas and particles, respectively; $T_1^* = T_1 + [(u_1 - u_2)^2 + (v_1 - v_2)^2]/2c_p$, $T_2^* = T_2$, $e_i = E_i + \delta_{1i}(p + \rho_i(u_i^2 + v_i^2)/2)$, E_i is the internal energy of unit mass of each phase.

The empirical coefficients f and g describing the momentum and energy transfer, respectively, between the phases are taken from [6].

Institute of Physics, Academy of Sciences of the Belorussian SSR, Minsk. Translated from Inzhenerno-Fizicheskii Zhurnal, Vol. 53, No. 1, pp. 32-37, July, 1987. Original article submitted April 22, 1986.

0022-0841/87/5301-0763$12.50

Numerical Scheme

The system in Eq. (1) is integrated in an Euler calculation grid with a number of cells which varies from layer to layer. This grid is constructed as follows: the flow field is successively cut into layers by planes perpendicular to the jet axis; the layes, in turn, are divided into cells at the points of intersection of the planes bounding them with flow tubes and the density discontinuities. The angle of rotation of the boundary of the flow tube in each subsequent step (layer) is found from the solution of the problem of the interaction between two semiinfinite ideal-gas flows over some unknown path [5]. This angle is evidently determined by equality of the pressures on both sides of the contact boundary: the maximum possible angles of rotation of the boundaries β_{max}^{out} and β_{max}^{in} are found at first, and then the desired angle β is found by successive halving of the sector obtained in the direction minimizing the modulus of the pressure difference on the two sides of the boundary.

So as to be specific, consider the lower flux (for the upper, all the angles are taken with the opposite sign), for which the angle of rotation of the gas is $\beta_p = \arctan(v/u) - \Delta$. If $\beta_p < 0$, the pressure at the given side of the boundary is determined from the formula for an expanding semiinfinite supersonic flow, i.e., for a Prandtl–Maier flow; if $\beta_p > 0$, however, the pressure at the boundary is found from the solution of the problem of symmetric supersonic flow around a wedge with a vertex angle $\chi = 2\beta_p$ [7]. In the latter case, as is known, the flow undergoes a discontinuity: a sloping density discontinuity appears, forming the wall of a new cell together with the boundaries of the flow tubes, within the framework of the given scheme. The angle of rotation of this discontinuity with respect to the jet axis is related in a known manner to the angle of slope of the contact discontinuity, and the hydrodynamic parameters behind the discontinuity are determined from the continuity laws at the sloping discontinuity. Such explicit separation of the discontinuities is physically justified, since it permits more correct separation of the fast processes — viscosity and heat conduction — determining the thickness of the discontinuities and the slow processes associated with phase interaction. Within the framework of the ideal-gas model used here, the discontinuity is regarded as infinitesimally thin, and since the numerical scheme applied does not spread it over several cells, there is no need to calculate flow tubes with large gradients of gasdynamic parameters. This ultimately gives the possibility of achieving satisfactory accuracy even when the jet itself and the cotraveling flow from the contact boundary to the region of unperturbed flow are represented by 20-30 flow tubes.

The difference equations corresponding to integral conservation laws with exchange terms for an individual calculation cell take the form

$$(\rho_i u_i h_r)^n = (\rho_i u_i h_r)_n + s^x_{n+1} - s^x_n - (\rho_i v_i h_z h_r/r)_n,$$

$$((\rho_i u_i^2 + \delta_{1i} p)\, h_r)^n = ((\rho_i u_i^2 + \delta_{1i} p)\, h_r)_n + \delta_{1i}\,(h_r p^x)_{n+1} - \delta_{1i}\,(h_r p^x)_n +$$
$$+ (u^x s^x)_{n+1} - (u^x s^x)_n - (\rho_i u_i v_i h_z h_r/r)_n - (h_z h_r f\,(u_j - u_i))_n, \qquad (2)$$

$$(\rho_i u_i v_i h_r)^n = (\rho_i u_i v_i h_r)_n + \delta_{1i} h_z (p^x_n - p^x_{n+1}) + (v^x s^x)_{n+1} - (v^x s^x)_n - (\rho_i v_i^2 h_z h_r/r)_n - (h_z h_r f\,(v_j - v_i))_n,$$

$$(e_i u_i h_r)^n = (e_i u_i h_r)_n + (s^x e^x/\rho^x)_{n+1} - (s^x e^x/\rho^x)_n - (e_i v_i h_z h_r/r)_n -$$
$$- [h_z h_r (g\,(T_j^* - T_i^*) + \delta_{1i} f\,((u_j - u_i)\, u_j + (v_j - v_i)\, v_i))]_n.$$

Here the subscript numbers the parameters when $z = z_0$, and the superscripts number those when $z = z_0 + h_z$; in addition, the symbols p^x_k, u^x_k, v^x_k, e^x_k, ρ^x_k and $s^x_k = \rho^x_k(u^x_k h_z - v^x_k h_t)$ denote parameters at the lower ($k = n$) and upper ($k = n + 1$) walls of the given cell. Since the particle parameters are determined in the same calculation grid as the gas parameters, strong numerical diffusion may appear at the edge of the region occupied by the particles. For its suppression, additional special cells are created at the edges of particle fields of each type; the upper walls of these cells are so-called separatrices: lines bounding the region of actual two-phase flow.

As well as the standard stability conditions for such explicit difference schemes [8], which for the given scheme must be formulated for both the gas and solid phase and imposed on the step along the jet axis, at least one other condition must be taken into account here: the longitudinal step must be less than the characteristic length for phase interaction ($L \approx \rho_i u_i / f$). In practice, however, the step is chosen to be even smaller, as a result of the requirements imposed on the accuracy of the specific calculations.

Discussion of the Results

The above numerical scheme is realized in a program which is used for numerous calculations in the following parameter ranges: the underexpansion varies from 0.1 to 10^6 and in some variants jet flow into vacuum is considered, with variation in the Mach number of the jet and the cotraveling flow in the range 2-7.5. The solid phase is taken to be Al_2O_3 particles of size 0.5-12 μm, and the mass flow rate is no more than 40% of the total mass of flow products. The initial parameters of the jet are specified either at the outlet or in the critical cross section of a Laval nozzle; in the second case, the calculation begins in the nozzle, and the particles may leave it in both molten and solid form. The concentration of liquid and solid phases in the particles is calculated from the law of energy conservation of the whole gas–particle system, disregarding the crystallization kinetics of Al_2O_3.

The interaction of particles with gas in a supersonic underexpanded jet issuing into a cotraveling flow may be represented qualitatively as follows. On leaving the nozzle, the gas-entrained particles turn by some characteristic angle at a distance of a few diameters from the nozzle outlet; this angle may be estimated within the framework of the method of plane cross sections [9]. Assuming that the longitudinal components of the gas and particle velocities do not vary greatly and are approximately equal, the following approximate equation is written for the separatrix of particles of radius R

$$\frac{4}{3}\pi R^3\rho_0\frac{d^2r}{dz^2}=\frac{1}{2}c_D\rho_1\pi R^2\left(\frac{v}{u}-\frac{dr}{dz}\right)^2 \tag{3}$$

with initial conditions specified in the cross section z = 0

$$r=r_0,\quad \frac{dr}{dz}=0. \tag{4}$$

Using the approximation proposed in [10] to describe the density and radial velocity of the gas in the jet in the region under the suspended discontinuity, and taking into account that the maximum angle of slope of the separatrix is approximately equal to its angle of slope with respect to the jet axis in the cross section where the particles are in the so-called central discharge wave, it is found that

$$\operatorname{tg}\theta\simeq\frac{\rho_1 r_0}{\rho_0}\frac{G}{RM(\gamma+1)}, \tag{5}$$

where R is the particle radius, μm; G is a constant, equal to $0.8\cdot10^5$ in the present case. As is evident from Fig. 1, this estimate is perfectly acceptable in the given range of parameters.

After turning through the given angle, the particles continue to move in an approximately constant direction and intersect the suspended density discontinuity close to the edge of the jet. The interaction increases somewhat here, and the particles, gradually turning and being decelerated by the gas, begin to collect in a characteristic annular spatial structure. The impact layer of gas, in turn, obtains some additional momentum from the direction of the jet axis and the first "barrel" is delayed in comparison with the case of pure gas. The deceleration effect is much intensified beyond the boundaries of the jet in the cotraveling flow, and here the tendency of the basic mass of particles to concentrate at the periphery appears most strongly: the particles move, as it were, in a "collecting lens" of gas, with a transverse velocity considerably less than that of the particles themselves. As a result, the spatial structure shown in Fig. 2a is formed. Here the axis of the two-phase jet issuing with M = 3 and underexpansion n = 20 in a cotraveling flow with Mach number M = 2 is directed from left to right, and the particles are distributed uniformly at the nozzle outlet.

The initial "spreading" of the particles over the jet and the annular structure obtained are clearly evident in Fig. 2a. Some nonmonotonicity in the region close to the nozzle outlet is evidently explained by interaction with the concentrated material beyond the suspended discontinuity. The particle temperature rapidly falls at first in the region under the suspended discontinuity (Fig. 2b). In strongly underexpanded jets and in jets issuing into vacuum, the phase interaction ultimately falls so much that "freezing" of the particle temperature occurs. In jets where the underexpansion is not especially large (n ≈ 5-15), "freezing" does not set in as a rule, and in addition, particles moving at large angles to the axis are heated for some limited time on reaching a region of dense cotraveling flow, where the longitudinal velocity of the gas undergoes a sharp discontinuity. For the sake of clarity, the jet and particle

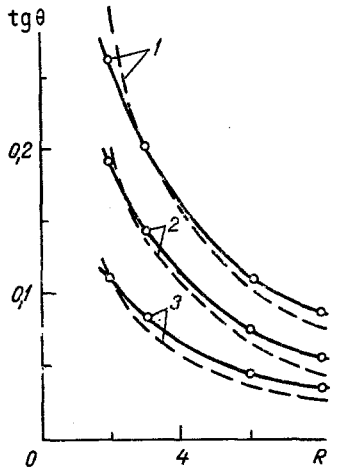

Fig. 1. Dependence of the slope of the separatrix with respect to the jet axis on the particle radius R, μm, the Mach number of the jet at the outlet M, and the adiabatic modulus of the gas γ obtained in numerical modeling (continuous curves) and from Eq. (5) (dashed curves): 1) γ = 1.2, M = 2; 2) 1.3, 3; 3) 1.4, 5.

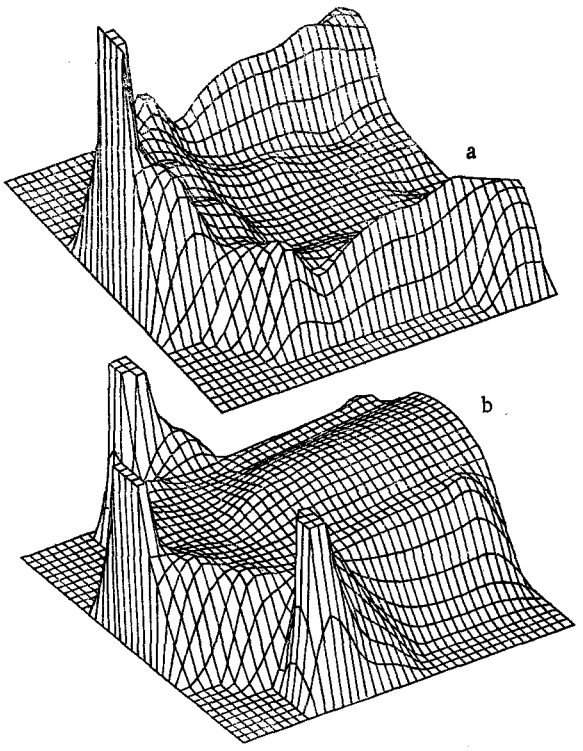

Fig. 2. Spatial distribution of the density (a) and temperature field (b) of the particles in a supersonic underexpanded jet issuing into a cotraveling flow.

parameters are chosen (underexpansion of the jet n = 15, initial gas temperature T = 2000°K, Mach number of jet M = 4.5, Mach number of cotraveling flow M = 2, particle radius R = 4 μm) so that the particles are not only heated on deceleration in the cotraveling flow to the melting point but also begin to melt; in Fig. 2b, this corresponds to two "peaks." Then the particles again solidify and rapidly cool.

Note, in conclusion, that this nonmonotonicity in the behavior of the density of the particle's spatial distribution and their temperature fields may be observed experimentally, in particular, in investigating light scattering at particles.

NOTATION

ρ_i, u_i, v_i, E_i, density, velocity components along the z and r axes, and internal energy of i-th phase, respectively; p, gas pressure; c_p, specific heat of gas at constant pressure; R, particle radius; θ, angle of rotation of particle separatrix; c_D, drag coefficient of spherical particle; ρ_0, density of particle material; r_0, nozzle radius, m; γ, adiabatic modulus; n, underexpansion of nozzle; ρ^x, u^x, v^x, p^x, gas parameters at side wall of cell; β_p, angle of rotation of side wall of cell with respect to axis; M, mach number of jet or cotraveling flow.

LITERATURE CITED

1. V. I. Blagosklonov and A. L. Stasenko, Uch. Zap. TsAGI, 8, No. 1, 32-42 (1977).
2. V. I. Blagosklonov, M. M. Glinskii, and A. L. Stasenko, in: Jet and Breakaway Flows [in Russian], Moscow (1979), pp. 95-105.
3. G. A. Saltanov, Nonequilibrium and Nonsteady Processes in Gas Dynamics [in Russian], Moscow (1970).
4. V. I. Kopchenov and A. N. Kraiko, Tr. Inst. Mekh. Mosk. Gos. Univ., No. 32, 96-108 (1974).
5. S. K. Godunov (ed.), Numerical Solution of Multidimensional Gas-Dyanmic Problems [in Russian], Moscow (1976).
6. D. Karlson and R. Khoglund, Raket. Tekh. Kosmonavt., 2, No. 11, 104-109 (1964).
7. L. D. Landau and E. M. Lifshits, Mechanics of Continuous Media [in Russian], Moscow (1954).
8. R. Courant, K. O. Friedrichs, and H. Lewy, Math. Ann., 100, 32-74 (1928).
9. G. Mairels and Dzh. Mullen, Raket. Tekh. Kosmonavt., 1, No. 3, 65-72 (1963).
10. K. P. Stanyukovich, Nonsteady Motion of a Continuous Medium [in Russian], Moscow (1971).

REGULAR AND STOCHASTIC DYNAMICS OF PARTICLES DURING VORTEX GENERATION IN A ROTATING STREAM WITH SHEAR

E. V. Guslyakova and A. A. Solov'ev

UDC 532.517.4

The results of an experimental study of the initial stage of development of a concentrated vortex are given.

Many practical problems of thermophysics and hydrodynamics require knowledge of the laws of organization of motions in vortex formations [1, 2]. There are a number of ways of exciting vortices [3], but it still remains unclear what physical processes occur in the initial stages of their formation. The mechanism of formation of concentrated vorticity in the presence of a trigger disturbance is well known [3]. During the further evolution of the initial disturbance and its conversion into a vortex, the character of the particle motion remains regular. A generation mechanism of an entirely different type, when a concentration of vorticity arises from random motions of particles, is possible in principle [4-7]. This regime of excitation of vortex formations has hardly been studied.

An installation was built to obtain and investigate vortices: a rotating cylindrical chamber, the flat bottom of which consists of a disk and two concentric rings [8]. The diameter of the installation is 0.46 m. The disk has a radius of 0.1 m, while the middle and outer rings have widths of 0.1 and 0.03 m, respectively. Water, rotating together with the vessel, fills it to a depth of 0.025 m. The liquid is subjected to the action of two opposite flows. They are created by clockwise rotation of the disk and counterclockwise rotation of both rings. The rings rotate at the same velocity, different from the velocity of the disk. The vessel as a whole rotates at the same velocity and in the same direction as the disk. The sign of rotation of the rings is arbitrarily taken as negative. The motions at the surface of the liquid were made visible by light scattering from microparticles moving along with the

State Oceanographic Institute, Moscow.

Translated from Inzhenerno-Fizicheskii Zhurnal, Vol. 53, No. 1, pp. 37-42, July, 1987. Original article submitted April 1, 1986.

0022-0841/87/5301-0767$12.50